Journal of Alloys and Compounds 509 (2011) 4154–4159

Contents lists available at ScienceDirect

Journal of Alloys and Compounds

journal homepage: www.elsevier.com/locate/jallcom

Preparation and characterization of Ni–P–nanoTiN electroless composite coatings

Liuhui Yu, Weigang Huang*, Xu Zhao

College of Materials Science and Engineering, Sichuan University, No. 24 South Section 1, Yihuan Road, Chengdu 610065, China

ARTICLE INFO

Article history:
Received 15 July 2010
Received in revised form 4 January 2011
Accepted 4 January 2011
Available online 12 January 2011

Keywords:
Coating materials
Surfaces and interfaces
Precipitation
Chemical synthesis
Microstructure
Mechanical properties

ABSTRACT

Ni–P–nanoTiN composite coatings were prepared successfully by electroless plating technique on AZ31 magnesium alloys. The composition, morphology, structure and phase transformation behaviour of the composite coatings were characterized respectively by using of scanning electron microscope (SEM), energy dispersive spectrometer (EDS) and X-ray diffractometer (XRD). The micro-hardness and wear resistance of the nano composite coatings, both in as-deposited and heat treated states, were investigated. The results demonstrated that the composite coatings, which contained nano TiN particles, exhibited much better properties in hardness and wear resistance than the conventional Ni–P coatings and original AZ31 magnesium alloys. These enhancements of properties are attributed to the nano TiN particles uniformly distributed in the Ni–P matrix.

1. Introduction

Magnesium and its alloys have extensive prospect for applications in automobile, aerospace, portable electronic appliances and biomedical devices, owing to their high strength to weight ratio, low density, high dimensional stability, high stiffness and recycling ability, etc. [1,2]. But the poor wear and corrosion resistances of magnesium and its alloy restricted their large-scale applications in industries [3,4]. This makes protective surface treatments an essential part of the manufacturing process for further application of magnesium alloys, which can provide a way of allowing the excellent properties of the substrate material to be maintained while protecting them against wear or corrosion [5–10].

Among the various surface treatments techniques, Ni–P electroless composite coatings are being increasingly used as a protective layer in numerous industrial applications for their unique properties such as wear and corrosion resistances, non-magnetism, improved micro-hardness and thickness uniformity [11–13]. Recently, it was found that the incorporation of finely dispersed nano solid particles into the Ni–P matrix, such as nano TiO_2, SiC and SiO_2 praticles, achieved by adding nano particles into the plating solution as a suspension during the deposition process, can significantly improve the properties of the composite coatings, especially in wear and corrosion resistances [14–17]. Owing to the superiority of both nano particles and Ni–P matrix, Ni–P electroless nano composite coatings are becoming the focus of widespread research.

Nano titanium nitride (TiN) particles have a high strength, high elastic modulus, and high hardness. Besides, the chemical and thermal stabilities of nano TiN particles are very high. Due to these properties, nano TiN particles are excellent candidate for Ni–P electroless composite coatings [18,19].

The aim of this work is to obtain Ni–P–nanoTiN coatings on AZ31 magnesium alloys by electroless plating process, and to investigate the composition, morphology, structure, micro-hardness and wear resistance of the composite coatings.

2. Experimental procedures

The substrate was AZ31 die cast magnesium alloys with a size of 10 mm × 10 mm × 10 mm. The nominal chemical composition of the alloys is given in Table 1. Prior to plating, all specimens were ground with 800 grit SiC abrasive paper to obtain surface of defined roughness. The specimens were then passed through the pretreatment as shown in Table 2. Due to the high chemical reactivity and potential differences between α-phase and β-phase, it is more difficult and complex to plate on AZ31 die cast magnesium alloys than other substrates [20]. To deal with this, fluoride acid was used to form a MgF_2 layer on the surface of the magnesium substrates, which could protect magnesium substrates from excess corrosion of plating bath and reduce the potential differences [21]. Immediately after the fluoride activation, the specimens were quickly transferred to the coating plating bath in a glass container placed in a constant temperature water bath to maintain the required temperature. The bath composition and other plating parameters used in this work are given in Table 3. For comparison, conventional Ni–P coatings were made with the same method.

* Corresponding author. Tel.: +86 28 85463766; fax: +86 28 85463766.
E-mail address: huangwg56@yahoo.com.cn (W. Huang).

0925-8388/$ – see front matter © 2011 Elsevier B.V. All rights reserved.
doi:10.1016/j.jallcom.2011.01.025

Table 1
Chemical composition of AZ31 magnesium alloys.

Composition	wt%
Al	3.10
Zn	1.20
Mn	0.50
Si	0.05
Cu	0.01
Ca	0.03
Mg	Balance

Table 2
Pre-treatment steps.

	Steps
1	Ultrasonic degreasing using acetone at 25 °C for 10 min
2	Rinse in NaOH (60 g/L) and Na_3PO_4 (20 g/L) at 70 °C for 10 min
3	Pickling in H_3PO_4 (60 mL/L), NH_4HF_2 (40 g/L) and H_3BO_4 (30 g/L) at 25 °C for 30 s
4	Fluoride activation in 40% hydrofluoric acid (375 mL/L) at 25 °C for 10 min

Table 3
Bath composition and plating parameters.

Plating bath composition	Concentration
$NiCO_3{\cdot}2Ni(OH)_2{\cdot}4H_2O$	12 g/L
$NaH_2PO_2{\cdot}H_2O$	22 g/L
Hydrofluoric acid (40%)	12 mL/L
NH_4HF_2	10 g/L
$C_6H_8O_7{\cdot}H_2O$	5 g/L
Ammonia solution (25%)	12 mL/L
H_2NCSNH_2	1 mg/L
Nano TiN particles	3 g/L
Operating conditions	
Temperature	80 °C
pH	6.5
Agitation	Supersonic wave stir
Time	4 h

Morphology of nano TiN particles was characterized by using a high resolving power transmission electron microscopy (HRTEM JEOL JEM 2010). The morphology, cross-section and wear surface of the composite coatings were examined by using a scanning electron microscopy (SEM JEOL JSM 5900L) coupled with energy dispersive spectroscopy (EDS). Heat treatments were performed on the Ni–P–nanoTiN coatings and Ni–P coatings in an air controlled furnace with pure argon atmosphere. The samples were annealed for 1 h each at 250, 300, 350, 400, 450 and 500 °C. The X-ray diffraction (XRD) patterns of the composite coatings before and after heat treatments were determined by using a Philips X'PERT MPD (Cu Kα radiation) diffractometer. The micro-hardness of both Ni–P coatings and Ni–P–nanoTiN coatings before and after heat treatments were evaluated by using a HXD-1000 micro-hardness tester at a load of 100 g and a duration of 15 s. Block-on-ring wear tests of original AZ31 magnesium alloys, Ni–P coatings and Ni–P–nanoTiN coatings were conducted at a normal load of 50 N and a sliding speed of 0.05 m s^{-1} by a MM200 tester. The wear losses were evaluated by electric balance with 0.001 mg accuracy.

3. Results and discussion

3.1. Morphology of nano TiN particles

Fig. 1 is the TEM image of nano TiN particles. From this image, it can be seen that the morphology of the TiN particles is close to spherical and the diameter in the range of 10–20 nm.

Table 4
Element composition of the Ni–P–nanoTiN coatings.

Element	at.%
Ni	86.76
P	11.73
Ti	01.51

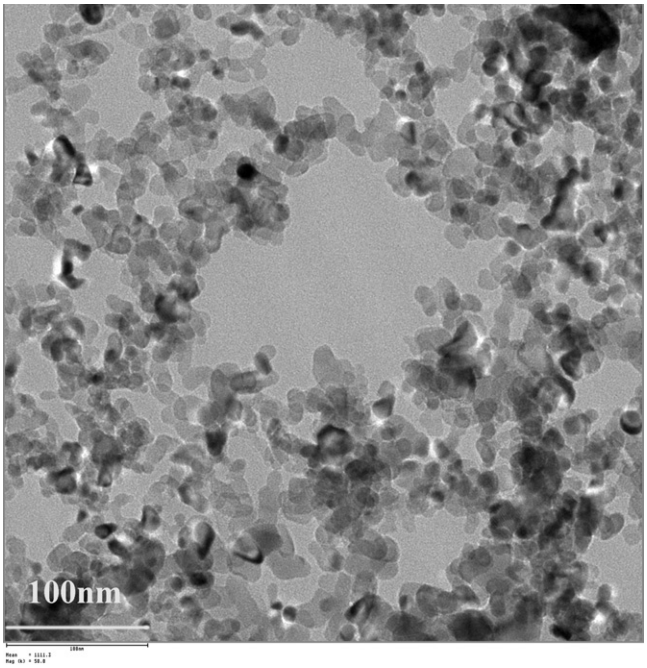

Fig. 1. TEM image of TiN nano-particles.

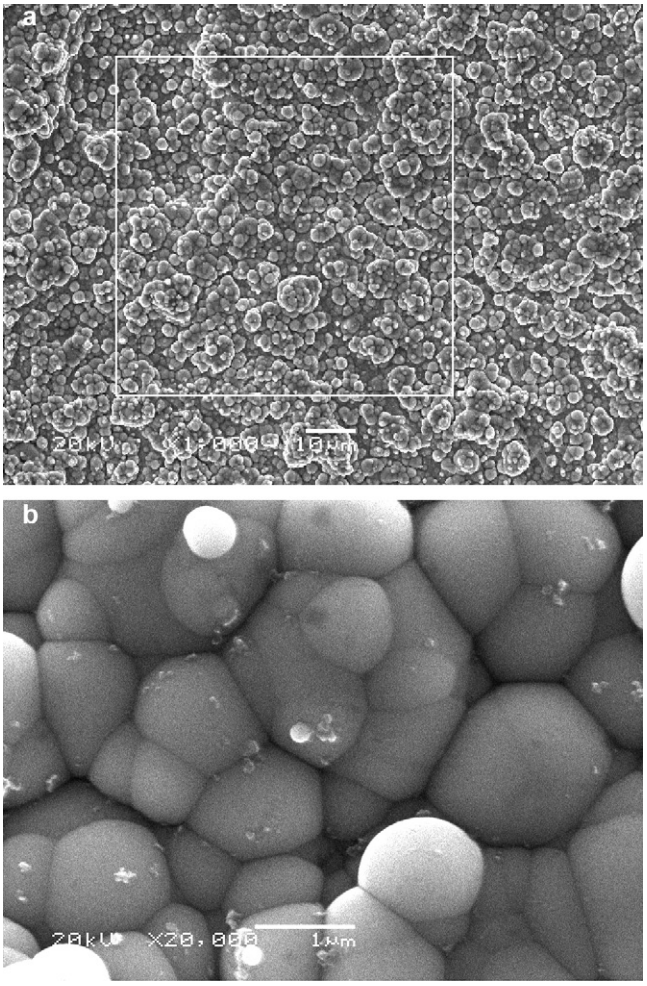

Fig. 2. Surface morphology of the same Ni–P–nanoTiN coatings with different magnification: (a) 1000×; (b) 20,000×.

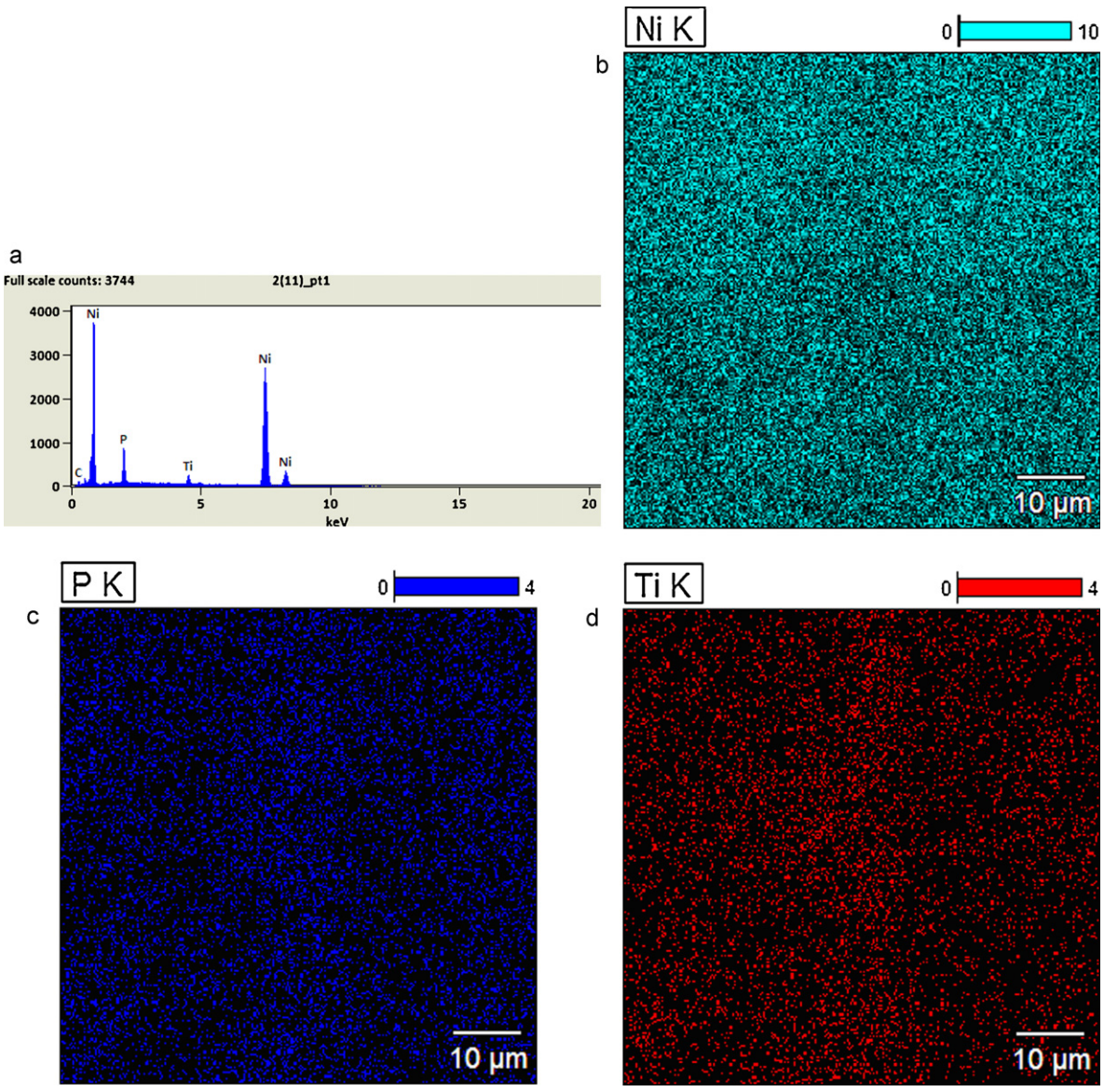

Fig. 3. EDS results of the surfaces showed in Fig. 2: (a) elements compositions; (b) elements map of nickel distribution; (c) elements map of phosphorus distribution; and (d) elements map of titanium distribution.

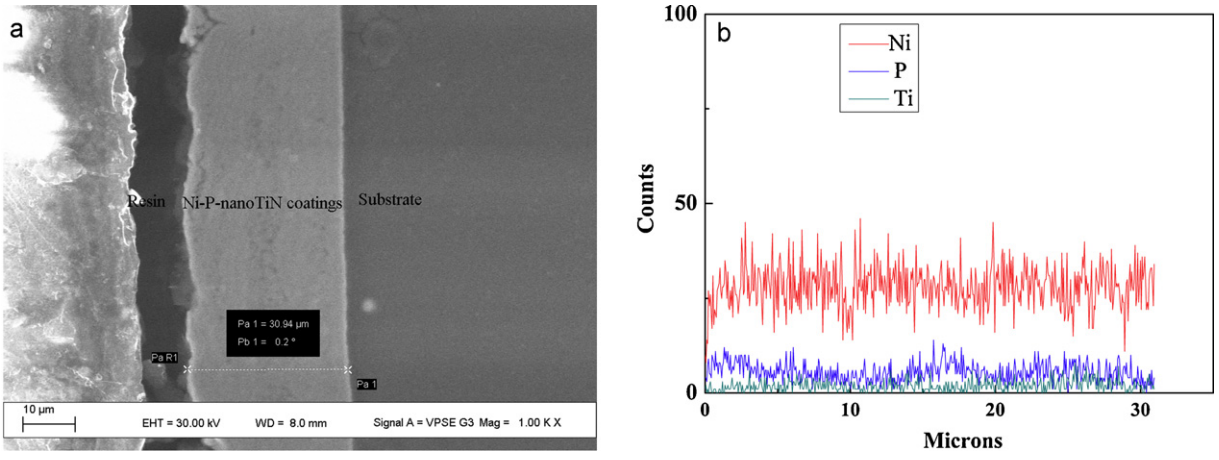

Fig. 4. SEM morphology and the corresponding EDS line scanning of the cross-section of Ni–P–nanoTiN coatings: (a) SEM morphology; (b) EDS line scanning.

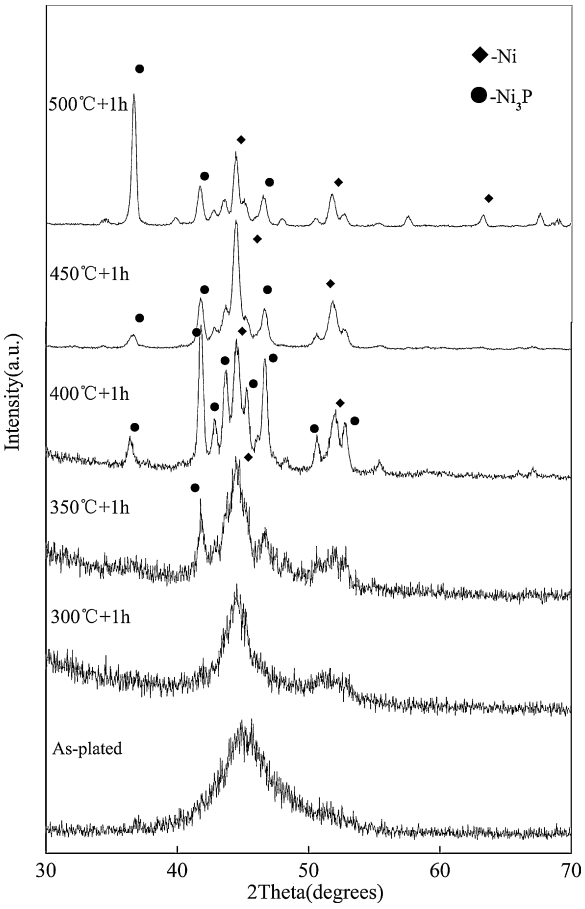

Fig. 5. XRD patterns of Ni–P–nanoTiN composite coatings before and after heat treated in argon atmosphere for 1 h at different temperatures (300, 350, 400, 450 and 500 °C).

3.2. Composition and morphology of composite coatings

Fig. 2(a) is the surfaces morphology of Ni–P–nanoTiN composite coatings, and Fig. 2(b) is the partial magnification of Fig. 2(a). It can be seen that the surfaces of the substrate were fully covered with the electroless coatings, and the composite coatings were composed of compact fine nodules uniform in size. Fig. 3(a) and Table 4 indicate that the major components on the surfaces of the composite coatings were 86.76 at.% nickel, 11.73 at.% phosphorus, and 1.51 at.% titanium. From the corresponding elements map as shown in Fig. 3(b)–(d), nickel, phosphorus, and titanium distributed uniformly on the surfaces of the composite coatings, indicating that the nano TiN particles uniformly distributed on the surfaces of the Ni–P matrix.

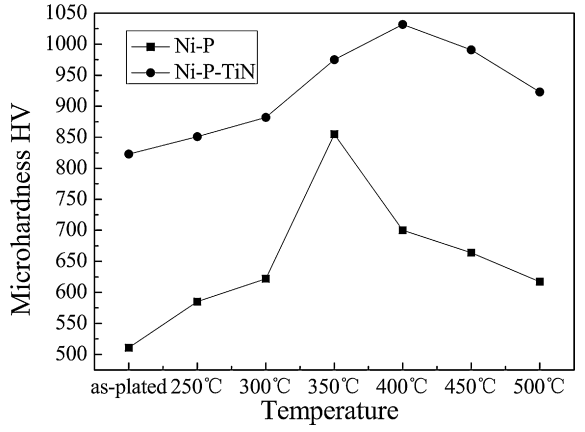

Fig. 6. The effects of heat treatment temperature on hardness of Ni–P and Ni–P–nanoTiN coatings.

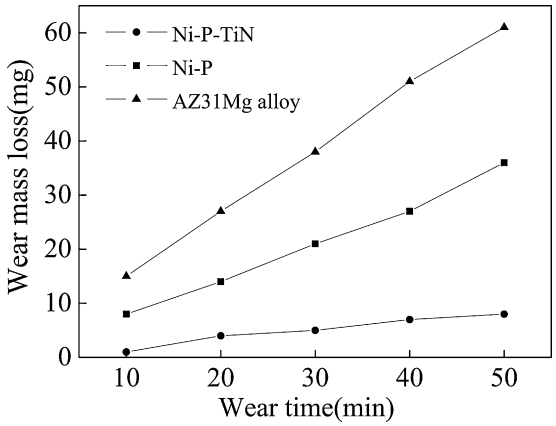

Fig. 7. The relationship between wear mass loss and wear time of magnesium alloys AZ31, Ni–P and Ni–P–nanoTiN coatings.

Fig. 4(a) is the cross-section morphology of the composite coatings. It shows that the inner was uniform and compact, without any pores or cracks. The average thickness of the coatings was approximately 30 μm. The corresponding EDS line scanning of Fig. 4(a) shows that the nickel, phosphorus and titanium distributed uniformly and longitudinally from the surface to the bottom of the composite coatings, which indicates that the nano TiN particles uniformly distributed in both surface and inner of the Ni–P matrix.

3.3. Structure of Ni–P–nanoTiN coatings before and after heat treatments

Fig. 5 presents XRD pattern of Ni–P–nanoTiN composite coatings before and after heat treatments. The broad diffraction peak at $2\theta = 40–50^{\circ}$ indicates that the as-plated composite coating had an amorphous structure. Even heated at 300 °C for 1 h, the microstructure of the composite coatings was still mainly amorphous. When the composite coatings were heated at 350 °C for 1 h, two kinds of crystalline diffraction peaks corresponding to Ni and Ni_3P phases were observed in the broadened amorphous matrix, which indicate that the composite coatings have begun to crystallize. When the heat temperature reached 400 °C, it was found that the diffraction peaks of both Ni and Ni_3P phases became much sharper, while the broadened amorphous matrix disappeared, indicating that the composite coatings were fully crystallized. Calculated by the Scherrer formula, the main grain sizes of the composite coatings heated at 400 °C, 450 °C, 500 °C are 19.5 nm, 24.7 nm, 27.5 nm respectively. These figures indicate the obvious grain coarsening of Ni and Ni_3P phases with the increasing heat temperature. As expected, on the basis of some literatures, the incorporation of nano TiN particles into the electroless Ni–P coating matrix did not visibly affect its structure [22].

3.4. Micro-hardness and wear resistance of Ni–P–nanoTiN coatings

Fig. 6 shows the micro-hardness of as-plated and heat treated Ni–P–nanoTiN coatings were significantly higher than the conventional Ni–P coatings. Apparently, the increase in micro-hardness of the composite coatings is attributed to the effect of dispersion strengthening generated by nano TiN particles. It was shown that the micro-hardness of both two kinds of coatings significantly

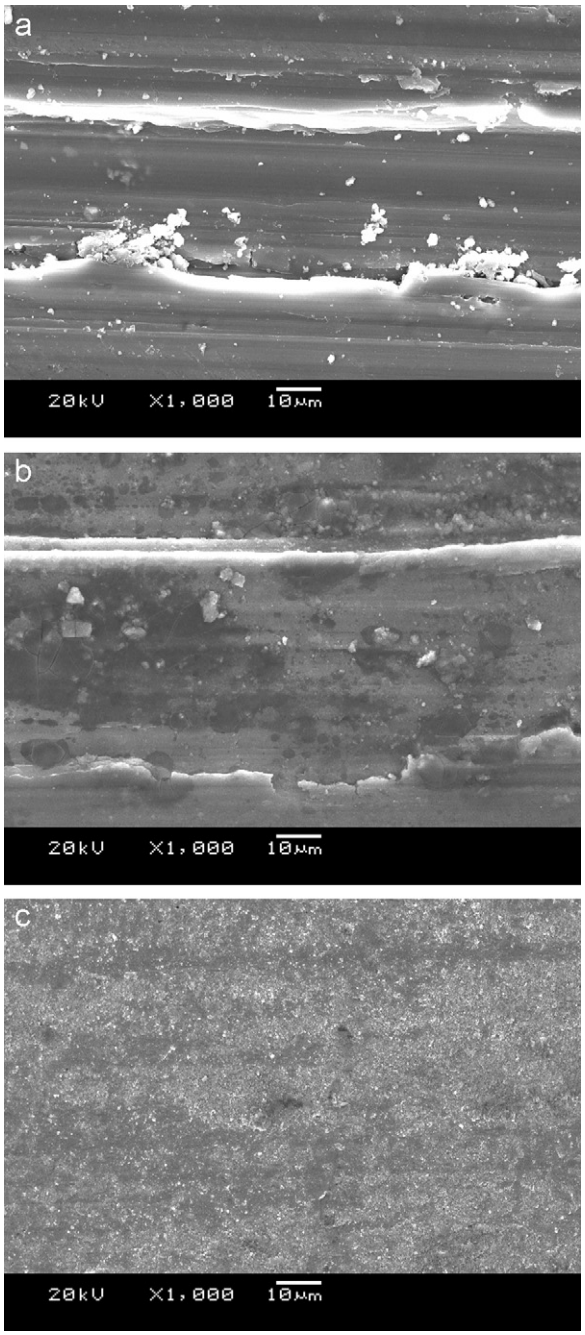

Fig. 8. SEM morphology of the worn surfaces: (a) AZ31 magnesium alloys; (b) Ni–P coatings; and (c) Ni–P–nanoTiN coatings.

increased after heat treatments, which is attributed to the formation and fine dispersion of the harden Ni_3P phases. When the Ni–P coatings and Ni–P–nanoTiN composite coatings were separately heated at 350 °C and 400 °C for 1 h, their micro-hardness reached the maximum, 855 HV and 932 HV respectively. Further increasing the heat temperature to 500 °C, the micro-hardness of both coatings decreased. This result must be related to the over aging of coatings which caused the grain coarsening of Ni and Ni_3P phases.

As shown in Fig. 7, the mass losses of AZ31 magnesium alloys, Ni–P and Ni–P–nanoTiN coatings all increased linearly with increase of the wear time. And the slopes of curves which represent the wear rate are obviously different. These figures show that the slope of AZ31 magnesium alloys was the largest among the three curves, which means the wear rate of AZ31 magnesium alloys was the highest, while the wear rate of Ni–P–nanoTiN coating was the lowest. After 50 min, the mass loss of AZ31 magnesium alloys reached nearly 60 mg, and the mass loss of Ni–P coating is 36 mg, while the mass loss of Ni–P–nanoTiN composite coatings is the minimal, only 8 mg.

For further analysis, all of the worn surfaces were examined by SEM. As shown in Fig. 8(a), the surface of AZ31 magnesium alloys was very rough, with typical abrasive and delamination wear features evidenced by deep ploughing furrows and numerous torn detachments. The worn surface of Ni–P coatings shown in Fig. 8(b) exhibited shallower furrows and slight scratches, which can be characterized as slight abrasive and adhesive wear. The worn surface of Ni–P–nanoTiN coatings was extremely smooth, only some pretty shallow grooves and slight scratches can be observed from Fig. 8(c), which indicated that only mild adhesive wear occurred. This excellent wear resistance of the Ni–P–nanoTiN composite coatings is attributed to the incorporation of nano TiN particles, which may delay the movement of dislocations and thus inhibit plastic deformation.

4. Conclusions

(1) The uniform Ni–P–nanoTiN coatings were successfully deposited uniformly on AZ31 magnesium alloys substrate by electroless plating after appropriate pretreatments for the substrate.
(2) The Ni–P–nanoTiN composite coatings were composed of compact fine nodules uniform in size without any pores or cracks, and the nano TiN particles uniformly distributed in the Ni–P matrix.
(3) The as-plated Ni–P–nanoTiN coatings had an amorphous structure. The Ni–P–nanoTiN coatings were fully crystallized at 400 °C, and the hardness of the Ni–P–nanoTiN coatings reached the highest at the same time.
(4) The introduction of nano TiN particles in the Ni–P matrix significantly improves the wear resistance compared with the conventional Ni–P coatings and original AZ31 magnesium alloys.

Acknowledgements

The author would like to thank Analysis and Testing Center of Sichuan University for all the helpful assistances in the experimental procedures. The author also gratefully acknowledges all the authors of references papers.

References

[1] F. Feyerabend, J. Fischer, J. Holtz, F. Witte, R. Willumeit, H. Drücker, C. Vogt, N. Hort, Acta Biomater. 6 (2010) 1834–1842.
[2] H.A. Patel, D.L. Chen, S.D. Bhole, K. Sadayappan, J. Alloys Compd. 496 (2010) 140–148.
[3] R.B. Alvarez, H.J. Martin, M.F. Horstemeyer, M.Q. Chandler, N. Williams, P.T. Wang, A. Ruiz, Corros. Sci. 52 (2010) 1635–1648.
[4] P. Li, M.K. Lei, X.P. Zhu, X.G. Han, C. Liu, J.P. Xin, Surf. Coat. Technol. 204 (2010) 2152–2158.
[5] A.S. Hamdy, M. Farahat, Surf. Coat. Technol. 204 (2010) 2834–2840.
[6] M. Zouari, M. Kharrat, M. Dammak, Surf. Coat. Technol. 204 (2010) 2593–2599.
[7] W.-J. Xi, N. Li, T. Zhang, W.-L. Zhu, H.-Z. Guo, J. Alloys Compd. 504S (2010) S414–S417.
[8] H. Mindivan, Surf. Coat. Technol. 204 (2010) 1870–1874.
[9] K.-C. Kung, T.-M. Lee, T.-S. Lui, J. Alloys Compd. 508 (2010) 384–390.
[10] A. Keyvani, M. Saremi, M.H. Sohi, J. Alloys Compd. 506 (2010) 103–108.
[11] G.-L. Song, Electrochim. Acta 55 (2010) 2258–2268.
[12] M. Raju, M.V. Ananth, L. Vijayaraghavan, J. Alloys Compd. 475 (2009) 664–671.
[13] J.N. Balaraju, Kalavati, K.S. Rajam, J. Alloys Compd. 486 (2009) 468–473.
[14] S. Ranganatha, T.V. Venkatesha, K. Vathsala, Appl. Surf. Sci. 256 (2010) 7377–7383.
[15] W. Chen, W. Gao, Y. He, Surf. Coat. Technol. 204 (2010) 2493–2498.

[16] F. Bigdeli, S.R. Allahkaram, Mater. Des. 30 (2009) 4450–4453.
[17] T. Rabizadeh, S.R. Allahkaram, Mater. Des. 32 (2011) 133–138.
[18] X. Guo, H. Yang, L. Zhang, X. Zhu, Ceram. Int. 36 (2010) 161–165.
[19] F.F. Xia, C. Liu, F. Wang, M.H. Wu, J.D. Wang, H.L. Fu, J.X. Wang, J. Alloys Compd. 490 (2010) 431–435.
[20] R. Ambat, W. Zhou, Surf. Coat. Technol. 179 (2004) 124–134.
[21] D. Guo, Z. Fan, Z. Yang, L. Zhao, P. Gao, Chin. J. Nonferrous Met. 17 (2007) 789–794.
[22] Y.S. Huang, X.T. Zeng, I. Annergren, F.M. Liu, Surf. Coat. Technol. 167 (2003) 207–211.